# Local magnetostriction measurement in a cobalt thin film using scanning probe microscopy

Kwang-Eun Kim, and Chan-Ho Yang

Citation: AIP Advances **8**, 105125 (2018); doi: 10.1063/1.5043466
View online: https://doi.org/10.1063/1.5043466
View Table of Contents: http://aip.scitation.org/toc/adv/8/10
Published by the American Institute of Physics

**Articles you may be interested in**

Deterministic domain reorientations in the $BiFeO_3$ thin film upon the thermal phase transitions
Applied Physics Letters **113**, 052904 (2018); 10.1063/1.5040726

Multiple relaxations of the cluster surface diffusion in a homoepitaxial $SrTiO_3$ layer
Applied Physics Letters **112**, 131602 (2018); 10.1063/1.5020943

Ferroelastic twin structures in epitaxial $WO_3$ thin films
Applied Physics Letters **107**, 252904 (2015); 10.1063/1.4938396

Disordered ferroelectricity in the $PbTiO_3/SrTiO_3$ superlattice thin film
APL Materials **5**, 066104 (2017); 10.1063/1.4986064

Domain switching in single-phase multiferroics
Applied Physics Reviews **5**, 021102 (2018); 10.1063/1.5018872

Perspective: Magnetoelectric switching in thin film multiferroic heterostructures
Journal of Applied Physics **123**, 240901 (2018); 10.1063/1.5031446

# Local magnetostriction measurement in a cobalt thin film using scanning probe microscopy

Kwang-Eun Kim[1] and Chan-Ho Yang[1,2,a]
[1]*Department of Physics and Center for Lattice Defectronics, Korea Advanced Institute of Science and Technology (KAIST), Daejeon 34141, Republic of Korea*
[2]*Institute for the NanoCentury, KAIST, Daejeon 34141, Republic of Korea*

(Received 9 June 2018; accepted 12 October 2018; published online 22 October 2018)

The local magnetostriction measurement has become an emerging issue because strain-mediated nanocomposites have received considerable attention due to their potential applications for high sensitivity sensors and high density energy harvesters. Compared to many instruments capable of measuring nanometric magnetic domains, techniques for measuring local magnetostriction have been rarely reported. Here, we introduce a local magnetostriction measurement method by modifying an atomic force microscope (AFM) by combing a solenoid to apply an external *ac* magnetic field and induce magnetostrictive excitation. The distribution of magnetostrictive response is mapped by contact mode AFM and lock-in detection techniques with a few nanometer lateral resolution. We have found that a few micrometer-size domains of a cobalt film showing different amplitude and phase signals of the magnetostrictive response are observed by the second-harmonic response of the *ac* magnetic field frequency, which is not detected in a linear response signal. We suggest that the phase and amplitude signals observed in each domain are related to magnetic-easy-axis directions. Our findings provide a unique pathway to understand the local magnetostrictive response based on scanning probe microscopy. © *2018 Author(s). All article content, except where otherwise noted, is licensed under a Creative Commons Attribution (CC BY) license (http://creativecommons.org/licenses/by/4.0/).* https://doi.org/10.1063/1.5043466

Magnetostriction is a property that changes the dimension of a material in response to the reorientation of magnetization in an external magnetic field.[1] Magnetostriction has its origin in the spin-orbit coupling in which the rotation of the magnetic moment induces the change of electron cloud resulting in lattice deformation.[2] Recently, understanding of the local magnetostrictive property has become an important issue for various applications requiring nanoscale manufacturing process such as biosensors, memory devices, and actuators.[3–5] For example, strain-mediated ferromagnetic-ferroelectric nanocomposites have been extensively studied for application to next-generation multiferroic memories due to their large magnetoelectric coefficients, and therefore measuring the local magnetostricive coefficient is required to test impairment of each memory bit.[6–10] However, the conventional magnetostriction measurements have been primarily performed to evaluate the macroscopic characteristics of the whole sample by using strain gauge, capacitance dilatometry, and optical interferometry.[11,12] Methodologies to measure local magnetostriction have been lacking compared to various instruments to observe local magnetic domain structures such as magnetic force microscopy (MFM), x-ray magnetic circular dichroism, Lorentz microscopy and magneto-optical microscopy.[13–18]

Here, we introduce a method to map the distribution of local magnetostrictive response based on scanning probe microscopy (SPM), that is called magnetostrictive force microscopy (MSFM). To activate a change of the sample thickness in an external *ac* magnetic field, a solenoid is necessarily combined with an atomic force microscope (AFM). Piezomagnetism and magnetostriction are characterized by first- and second-order coupling between the magnetic moment and mechanical

[a]E-mail: chyang@kaist.ac.kr

 © Author(s) 2018

strain.[19,20] Magnetostriction is described as,

$$\frac{3}{2}\lambda_s(1-\cos^2\theta), \tag{1}$$

where $\lambda_s$ is the saturation magnetostriction coefficient, and $\theta$ is the angle between the direction of domain magnetization and that of magnetic field.[21] Equation (1) is an expression for representing magnetostriction of a bulk sample without external strain. In the case of ferromagnetic films, the in-plane deformation can be restricted by the clamping effect of the substrate, which also affects out-of-plane deformation. Therefore, Eq. (1) can vary depending on the geometry of the sample. In this paper, the surface oscillation by the sample thickness change is detected at only second harmonic frequency (2ω) of the *ac* magnetic field for the magnetostrictive detection. In terms of the contact force measurement using an AFM tip, MSFM is conceptually similar to piezoresponse force microscopy (PFM) extensively used to measure the nanoscale converse piezoelectric response. The working principle of PFM is to apply an external *ac* electric field into a piezoelectric material, after which the deformation of the sample is measured through the tip in contact with the sample surface and lock-in detection technique.[22] The differences between MSFM and PFM are that an external *ac* magnetic field is applied to the ferromagnetic sample and the sample deformation oscillating at 2ω is measured. Although there are a few efforts to measure the magnetostrictive response using probe techniques,[23–25] mapping the distribution of the magnetostrictive response with nanoscale spatial resolution in ferromagnetic thin films has not been reported yet. Especially, amplitude and phase signals measured by lock-in detection contain important physical information such as polarization directions and electrostatic potentials in SPM-based electric measurements, but understanding of the magnetostrictive responses is still veiled.[26,27] In the followings, we introduce a design of MSFM based on the commercial AFM combining an external *ac* magnetic field generator. By using the equipment, we explore the magnetostrictive property on a 200-nm-thick cobalt metal thin film, thereby recognizing the boundary of two domains showing different magnetostrictive responses. Finally, we suggest a possible scenario to interpret the magnetostrictive responses in relation to magnetic-easy-axis directions.

Our MSFM is designed based on a commercial AFM (MultiMode-V, Bruker). The MSFM is the sensitive instrument for measuring changes in sample thickness of several pm. If we apply a magnetic field to the whole AFM system using a Helmholtz coil, unintended deformations will occur in various components that make up the AFM. In this reason, a magnetic field should be concentrated on the ferromagnetic sample using a small magnetic field generator. In most commercial AFMs, a spacer is needed to secure the space for a solenoid because of their compact design, as shown in Fig. 1(a). To shield the vibration noise which can be generated from the solenoid, the solenoid is suspended on the spacer to be physically isolated from the scanner, and a four-lagged sample stage mounted on the scanner does not directly contact with the solenoid. The solenoid is placed so that its apex is as close to the sample as possible. It enables a direct application of a strong magnetic field to the sample thickness direction through a hole in the center of the sample stage. A permalloy core with a sharp endpoint is inserted in the center of the solenoid to amplify and concentrate the magnetic field. The solenoid is designed in a small size with a height of 2 cm and this is manufactured to be mounted on a commercial AFM as an external module, which is easily detachable. Details of the MSFM design are shown in Fig. S1. The specific working principle of MSFM is as follows: MSFM is based on the contact mode AFM to measure the surface deformation of a ferromagnetic sample when the sample is subjected to a magnetic field. Using a current source, an *ac* current is applied to the solenoid and simultaneously phase information of the *ac* current is passed on to a lock-in amplifier as a reference signal. The induced *ac* magnetic field results in deformation of the sample thickness by a Joule effect – magnetostriction oscillating at 2ω of the *ac* magnetic field frequency. The magnetostriction response is transmitted to the tip in contact with the sample surface, and the vibration of the cantilever is converted to electrical signals by using a position-sensitive detector capable of tracking laser beam reflection. Finally, amplitude and phase information of the magnetostrictive response is analyzed by lock-in detection.

We measured the magnetic field strength using a gauss meter (GMO8, HIRST Magnetic Instruments Ltd.) at the sample stage without the ferromagnetic sample. The magnetic field linearly

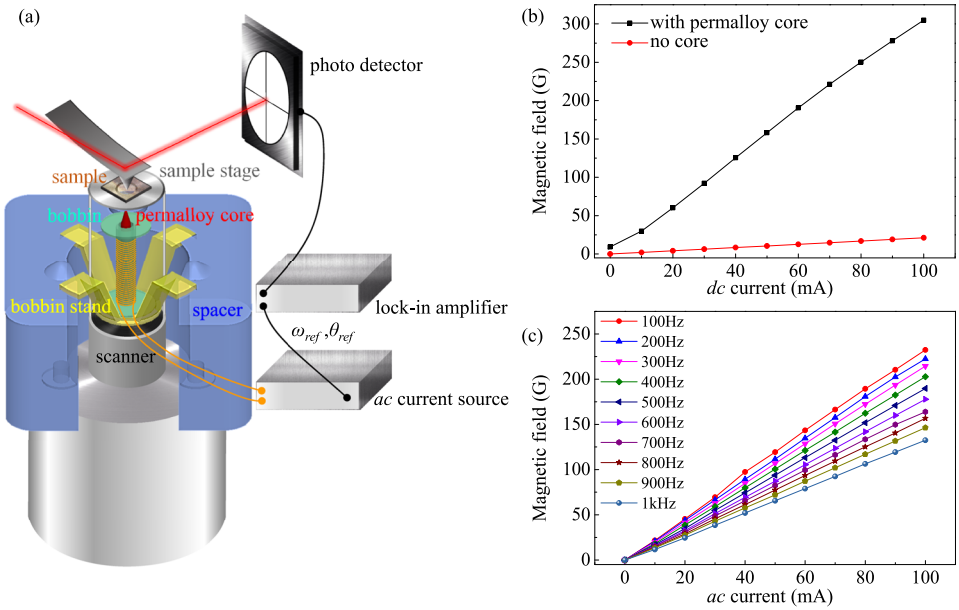


FIG. 1. (a) The geometry of the MSFM. The height of the space (blue color) and bobbin (mint color) are 22 mm and 20 mm, respectively. The bobbin stand (yellow color) is hung on the spacer, and the bobbin is placed on the bobbin stand. The inner diameter of the bobbin is 3 mm, and a permalloy rod (red color) with a diameter of 2 mm and sharp end point is inserted as a magnetic core. The pointed shape of the permalloy core serves to focus magnetic fields. To make the solenoid, the enamel wire with a diameter of 0.15 mm is wound in the bobbin 1000 times. The enamel wire is connected to the *ac* current source, and the phase marker signal of the current source and the photodetector signal are connected to the lock-in amplifier. (b) Measured magnetic field versus input *dc* current with/without the permalloy core. (c) Measured *ac* magnetic field versus input *ac* current with the permalloy core. As the *ac* current frequency increases by 100 Hz, the magnitude of magnetic field decreases by about 10 gauss.

increases in proportion to the magnitude of current, and the permalloy core amplifies the magnetic field 15 times, as shown in the Fig. 1(b). The magnitude of the magnetic field decreases by 10 G, as increasing the frequency of the *ac* current by 100 Hz (Fig. 1(c)). The decrease in the magnetic field amplitude can be attributed to the induced current generated by applying an *ac* current to the coil. The total current flowing through the coil can be expressed as the sum of the applied *ac* current ($I$) and induced current ($\Delta I$), and the two currents flow in opposite directions each other. Because the induced current increases in proportion to the frequency of the *ac* current and as a result the amount of total current flowing through the coil decreases, MSFM operates at low frequency *ac* currents, limiting the scan speed of MSFM. The induced current $\Delta I$ is estimated by the following equation:

$$\Delta I = \frac{\varepsilon}{\Omega} = -N\frac{\Delta B \cdot S}{\Delta t \cdot \Omega} = -1000\frac{430\,\mathrm{G} \cdot \pi \cdot (2.5 \times 10^{-3} m)^2}{0.01\,\mathrm{sec} \cdot 27\,\Omega} = -3.1\,\mathrm{mA}, \quad (2)$$

where $\varepsilon$ is the induced electromotive force, $\Omega$ is the resistance of the solenoid, $N$ is the number of wire wraps, and $S$ is the cross sectional area of the solenoid. The 430 G is estimated by two times of the root-mean-square value of an *ac* magnetic field with an amplitude of 305 G (This 305 gauss is measured when a *dc* current of 100 mA is applied to the coil). The negative sign means the opposite direction of the applied current direction. In the Fig. 1(b), the magnetic field increases by 30 G as increasing the current by 10 mA, thus it is reasonable that the magnetic field is reduced by 10 G due to the induced current of -3.1 mA. In our experiments, we applied an *ac* magnetic field of the 220 G amplitude to the cobalt film. Applying a magnetic field above the coercive field is a minimum requirement to obtain the magnetostrictive response considering the known coercive field of the cobalt film, ~100 G.[28]

We analyze the 200-nm-thick cobalt film with a 3-nm-thick TiN as a capping layer grown by sputter deposition on a Si $(100)_{pc}$ substrate. First, we measured the MSFM on a 3 nm thick TiN film

grown on a Si substrate to investigate the null effect and estimate the noise level, as shown in Fig. S2. From the amplitude and phase images, the amplitude noise level is estimated to be less than 0.5 pm with random phase signals. Since the typical MSFM signal level in the cobalt film is a few pm, that is clearly beyond the noise level. Cobalt metal exhibits a large magnetostriction coefficient among pure elements at room temperature, and the saturation magnetostriction is known to be $\lambda_s = -62 \times 10^{-6}$.[29] From the topographic image in Fig. 2(a), the entire film is uniformly deposited with 2.2 nm roughness, thus MSFM signals are likely unrelated to a crosstalk with surface topography. The tip scan speed is 0.8 μm/s, and a pixel size of the image is 30 nm × 30 nm. We use silicon bare tips (NSC35, MikroMasch), one pixel size is large enough comparing the radius of the tip end (typically ~ 8 nm). While the tip runs across one pixel length, the tip is expected to vibrate approximately 10 times at a magnetic field frequency of 250 Hz due to the magnetostrictive effect. Comparing to conventional *ac* measurements in SPM operating from ~kHz to ~MHz, MSFM operates at significantly lower frequencies associated with an *ac* magnetic field frequency at hundreds of Hz. Because of the low operating frequency of MSFM, the MSFM signal is significantly affected by the tip scanning speed (Fig. S3 in the supplementary material). In principle, the spatial resolution can be improved up to the tip diameter size by reducing the measuring image size and the scan speed.

The amplitude of the magnetostrictive response was calibrated in the unit of length by performing a general calibration procedure based on the static force-distance curve. The force-distance curve is a plot of the deflection of the cantilever versus the height extension of the piezoelectric scanner as shown in Fig. S4. In our SPM case, the position-sensitive photo detector has a sensitivity of 0.027 V/nm. Using this sensitivity value, the voltage value obtained from the MSFM measurement can be converted in the unit of length.

Two regions are recognized in the amplitude and the phase images (Fig. 2(b) and (c)). The left macro-domain has a strong magnetostrictive signal, however the right domain shows almost zero strength of the response. It indicates the two domains have different magnetic easy axes. We can

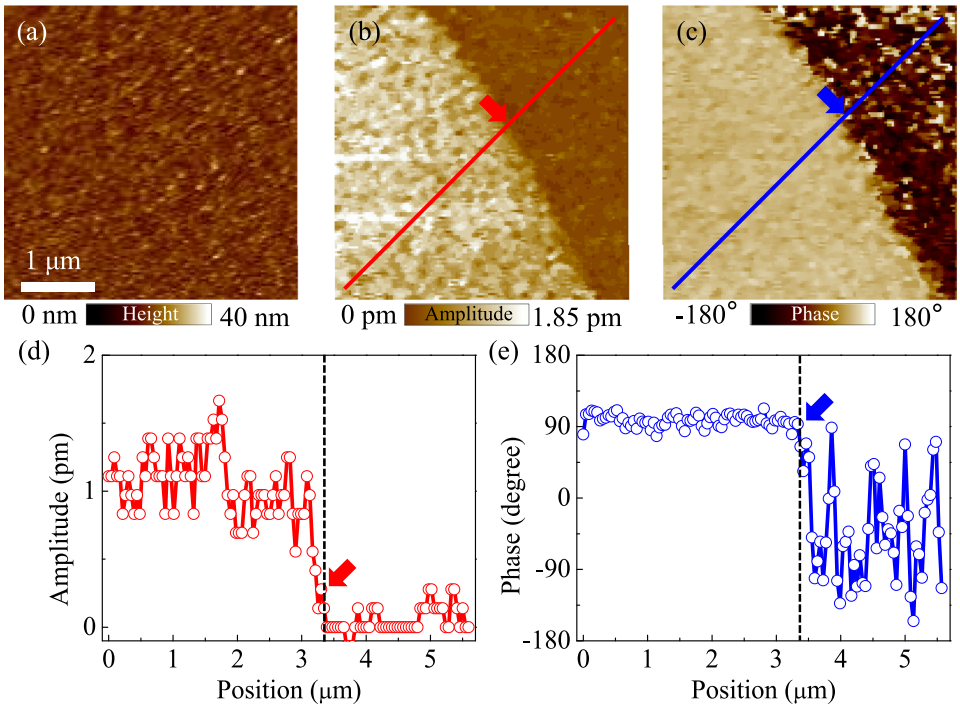


FIG. 2. Mapping magnetostrictive responses on a cobalt thin film. (a) Topography, (b) amplitude, and (c) phase images. An *ac* current of 250 Hz and 100 mA is applied to the coil, and all images are acquired simultaneously with a single scan. (d) and (e) Amplitude and phase cross sections showing the signal change around the domain wall taken at positions of red and blue lines in (b) and (c), respectively. Arrows point to the boundary area between two domains in the cross section line.

presume the magnetic easy axes considering magnetostriction is maximized when the external magnetic field is perpendicular to the magnetization, suggesting the left domain has in-plane magnetizations and the right domain has out-of-plane magnetizations. We note that the domain with the strong signal shows a phase shift by amount of +90°. We will further discuss the relation between amplitude and phase signals later in this paper. It is thought that the observed domains are macro-domains consisting of fine stripe 180∘ magnetic domains that are often found in similarly thick cobalt films and the width of the stripe domains has been reported to be of an order of a few 100 nm.[30] Nevertheless, we couldn't detect the existence of any fine stripes in the MSFM images. It is because magnetostriction is a quadratic effect of magnetization and the magnetostrictive response cannot distinguish such 180∘ magnetic domains.[31] But, we can identify the fine stripe domains using the conventional MFM (Fig. S5 in the supplementary material). In cobalt thin films with film thickness above 8 Å, magnetic moment is expected to align to in-plane directions due to the magnetostatic interaction while the magnetic moment for the film thickness less than 8 Å is normal to the film surface by surface anisotropy.[32] But, in our sample case, non-zero out-of-plane directional component of magnetization is detected in a large macro-domain and thus fine stripes are sensible by using the MFM. The macro-domain with stripes corresponds to the region with the weak MSFM signal (Fig. S6 in the supplementary material).

We investigated the magnetostrictive response versus the magnetic field strength over another region in the same sample, as shown in the Fig. 3. Because MSFM can sense the deflectional vibration of the tip as much as 0.5 pm through the lock-in detection technique, the magnetostictive response of a few pm is detectable. The amplitude of the magnetostrictive response is measured up to about 3 pm. Considering the 200-nm thickness of the cobalt film and the saturated magnetostriction value of the cobalt metal known as $-62 \times 10^{-6}$,[29] the expected magnetostriction value is ~ 12 pm. We consider

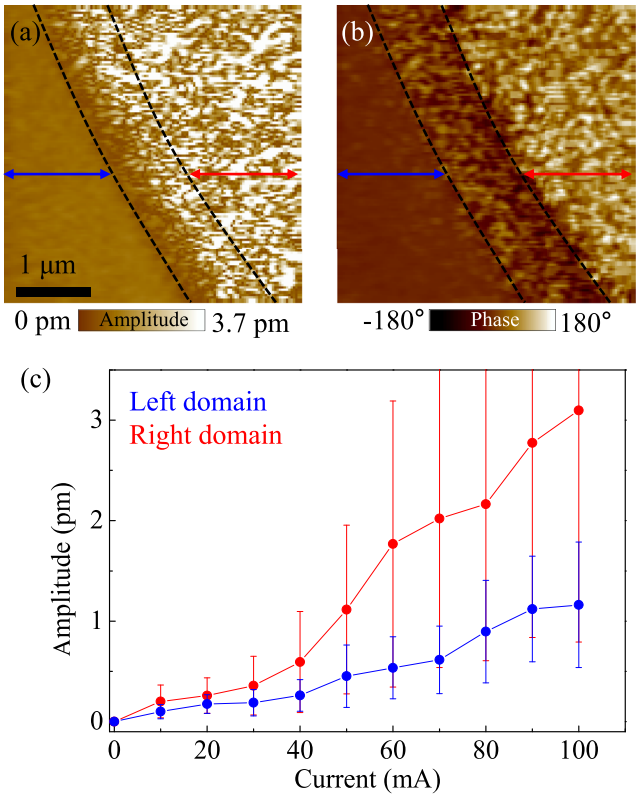


FIG. 3. Comparison of magnetostrictive responses in two distinguished domains. (a) Amplitude and (b) phase images acquired simultaneously by a single scan. An *ac* current of 100 mA at 250 Hz was applied to the coil. Blue and red arrows represent left and right domain regions, respectively. (c) Amplitude curves of magnetostrictive response versus applied *ac* current in each domain. Error bar is the standard deviation of measured data.

that the larger magnetic field is required to obtain the saturated magnetostriction value. Moreover, when the magnetic easy axis is out of parallel with the surface plane of the film, magnetostriction value can be measured lower than the expected value because the magnetostriction value is largest when the magnetic field is perpendicular to the easy axis (Eq. (1)).[21] Based on the magnitude of the magnetostrictive response, we estimated that magnetic easy axis in the right domain is more parallel to the surface plane comparing to the left domain. The intermediate domain with a width of ~ 1μm is observed between the two domains.

The cobalt metal has a negative magnetostrictive property that the material shrinks in the direction of the magnetic moment. When one period of the magnetic field is applied as a sinusoidal waveform, the sample oscillates twice in the thickness direction. In the real system, the domain wall motion complicates the situation because the magnetic field is macroscopically applied to the sample. When an external magnetic field is applied to the ferromagnetic material, the magnetic moment is aligned by competition between magnetostatic energy and magnetocrystalline anisotropy energy. For example, if magnetic easy axis is parallel to the magnetic field direction, the domain walls move to increase the size of domain lying parallel to the magnetic field to reduce the magnetostatic energy and maintain magnetocrystalline anisotropy energy. On the other hand, if magnetic easy axis is perpendicular to the magnetic field, the magnetic moments of an entire domain will rotate to the magnetic field direction because the domain wall motion is insufficient for lowering the magnetostatic energy. In this case, magnetocrystalline anisotropy energy increases, but when the magnetic field is large enough, the magnetic moment rotates to reduce the magnetostatic energy. Therefore, when the magnetic easy axis is perpendicular to the magnetic field direction, the large magnetostrictive response signal is observed, while the magnetic easy axis is parallel to the magnetic field direction, the magnetostrictive response signal becomes smaller through the domain wall motion.

Figure 4 shows the relation between the direction of magnetic easy axis and phase difference. For three cases: (1) when the magnetic easy axis lies parallel to the surface plane, the sample thickness is in the most elongated state. In this case, the sample thickness always decreases under the magnetic field. When considering the motion of the probe, the probe draws a sinusoid with the 2ω frequency and +90° phase difference (Fig. 4(a)). (2) When the magnetic easy axis lies in the sample thickness direction, the domains where the magnetic moment is parallel to the magnetic field become wider by

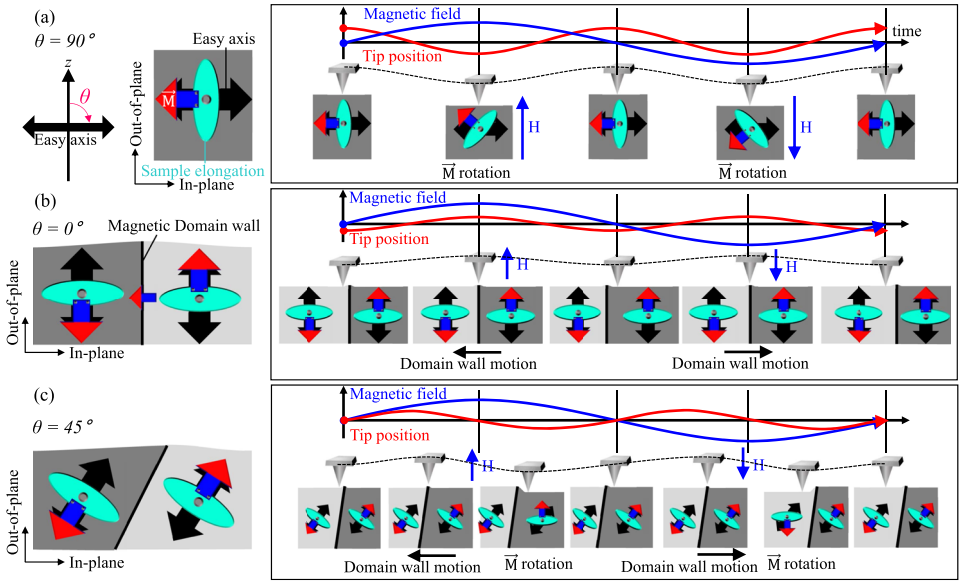


FIG. 4. A proposed scenario to interpret the amplitude and phase difference of the magnetostrictive response, when the magnetic easy axis lies (a) 90°, (b) 0°, and (c) 45° to the magnetic field. The schematics depict the oscillation of the tip by magnetic domain wall motion and magnetic moment ($\vec{M}$) rotation in response to the *ac* magnetic field measured at a fixed position.

the domain wall motion.[33] Considering the rotation of the magnetic moment at the domain wall, the sample thickness in the vicinity of the domain wall can be slightly elongated comparing the domain area by rotation of magnetic moments in the Bloch wall. In this case, the probe draws a sinusoid with the 2ω frequency and -90° phase difference (Fig. 4(b)). (3) When the magnetic easy axis is obliquely placed with respect to the sample thickness direction, the domain wall motion and the rotation of the magnetic moment are combined. The domains more parallel to the magnetic field are widened by the domain wall motion, after which the magnetic moment is rotated to the magnetic field direction. In this case, the probe draws a sinusoid with the 2ω frequency and zero phase difference (Fig. 4(c)). According to our scenario, as the magnetic easy axis becomes more parallel (perpendicular) to the film surface plane, the phase difference approaches +90° (-90°). In Fig. 2, it is reasonable that the phase 90° domain shows the larger magnetostrictive response than that of the phase -90° domain, whereas because of the weak magnetostriction amplitude signal in the upper right domain, the probe often fails to read the magnetostrictive phase response, causing fluctuation in the phase contrast.

In summary, we reported on the local measurement of magnetostriction using MSFM. Using the external *ac* magnetic fields, we activate the magnetostrictive response of a magnetic film. Through phase difference and amplitude information analysis, we estimated the direction of magnetic easy axis. The specific MSFM design and the analysis method of the magnetostrictive response provide an important cornerstone to the research of local magnetostriction.

See supplementary material for details of the MSFM design, the MSFM measurement result of the 3 nm thick TiN film, MSFM images measured with different scan speeds, a force-distance curve, large area MFM images, and MFM and MSFM images measured in an identical area.

This work was supported by the National Research Foundation (NRF) Grant funded by the Korean Government via the Creative Research Initiative Center for Lattice Defectronics (2017R1A3B1023686).

[1] G. Engdahl, *Handbook of giant magnetostrictive materials* (Academic Press, San Diego, 1999), Chap. 1.
[2] R. Wu, J. Appl. Phys. **91**, 7358 (2002).
[3] L. Fu, S. Li, K. Zhang, I.-H. Chen, V. A. Petrenko, and Z. Cheng, Sensors **7**, 2929 (2007).
[4] V. V. Kokorin and M. Wuttig, J. Magn. Magn. Mater. **234**, 25 (2001).
[5] A. Ludwig and E. Quandt, J. Appl. Phys. **87**, 4691 (2000).
[6] H. Zheng, J. Wang, S. E. Lofland, Z. Ma, L. Mohaddes-Ardabili, T. Zhao, L. Salamanca-Riba, S. R. Shinde, S. B. Ogale, F. Bai, D. Viehland, Y. Jia, D. G. Schlom, M. Wuttig, A. Roytburd, and R. Ramesh, Science **303**, 661 (2004).
[7] H.-J. Liu, L.-Y. Chen, Q. He, C.-W. Liang, Y.-Z. Chen, Y.-S. Chien, Y.-H. Hsieh, S.-J. Lin, E. Arenholz, C.-W. Luo, Y.-L. Chueh, Y.-C. Chen, and Y.-H. Chu, ACS Nano **6**, 6952 (2012).
[8] S. Ojha, W. C. Nunes, N. M. Aimon, and C. A. Ross, ACS Nano **10**, 7657 (2016).
[9] M. Gao, R. Viswan, X. Tang, C. M. Leung, J. Li, and D. Viehland, Sci. Rep. **8**, 323 (2018).
[10] D. H. Kim, N. M. Aimon, and C. A. Ross, APL Mater. **2**, 081101 (2014).
[11] N. B. Ekreem, A. G. Olabi, T. Prescott, A. Rafferty, and M. S. J. Hashmi, J. Mater. Process. Technol. **191**, 96 (2007).
[12] H. Samata, Y. Nagata, T. Uchida, and S. Abe, J. Magn. Magn. Mater. **212**, 355 (2000).
[13] T. Shinjo, T. Okuno, R. Hassdorf, K. Shigeto, and T. Ono, Science **289**, 930 (2000).
[14] H. Hopster and H. P. Oepen, *Magnetic microscopy of nanostructures* (Springer, Berlin, 2005), Chap. 1.
[15] J. McCord, J. Phys. D: Appl. Phys. **48**, 333001 (2015).
[16] N. O. Urs, B. Mozooni, P. Mazalski, M. Kustov, P. Hayes, S. Deldar, E. Quandt, and J. McCord, AIP Adv. **6**, 055605 (2016).
[17] J. H. Lee, B.-K. Jang, K. R. Kang, D.-J. Kim, B.-G. Park, and C.-H. Yang, Phys. Rev. B **97**, 104420 (2018).
[18] B.-K. Jang, J. H. Lee, K. Chu, P. Sharma, G.-Y. Kim, K.-T. Ko, K.-E. Kim, Y.-J. Kim, K. Kang, H.-B. Jang, H. Jang, M. H. Jung, K. Song, T. Y. Koo, S.-Y. Choi, J. Seidel, Y. H. Jeong, H. Ohldag, J.-S. Lee, and C.-H. Yang, Nat. Phys. **13**, 189 (2017).
[19] Q. N. Chen, F. Ma, S. Xie, Y. Liu, R. Proksch, and J. Li, Nanoscale **5**, 5747 (2013).
[20] C.-G. Stefanita, *From bulk to nano: the many sides of magnetism* (Springer, Berlin, 2008), Chap. 3.
[21] S. Chikazumi, *Physics of ferromagnetism* 2nd Ed. (Oxford University Press, New York, 1997), Chap. 14.
[22] E. Soergel, J. Phys. D: Appl. Phys. **44**, 464003 (2011).
[23] R. A. Brizzolara and R. J. Colton, J. Magn. Magn. Mater. **88**, 343 (1990).
[24] A. C. Papageorgopoulos, H. Wang, C. Guerrero, and N. Garcia, J. Magn. Magn. Mater. **268**, 198 (2004).
[25] J. J. Park, E. C. Estrine, S. M. Reddy, B. J. H. Stadler, and A. B. Flatau, J. Appl. Phys. **115**, 17A919 (2014).
[26] K.-E. Kim, B.-K. Jang, Y. Heo, J. H. Lee, M. Jeong, J. Y. Lee, J. Seidel, and C.-H. Yang, NPG Asia Mater. **6**, e81 (2014).
[27] K.-E. Kim, S. Jeong, K. Chu, J. H. Lee, G.-Y. Kim, F. Xue, T. Y. Koo, L.-Q. Chen, S.-Y. Choi, R. Ramesh, and C.-H. Yang, Nat. Commun. **9**, 403 (2018).
[28] H. Luo, D. Wang, J. He, and Y. Lu, J. Phys. Chem. B **109**, 1919 (2005).

[29] K. B. Hathaway and A. E. Clark, MRS Bull. **18**, 34 (1993).
[30] M. Hehn, S. Padovani, K. Ounadjela, and J. P. Bucher, Phys. Rev. B **54**, 3428 (1996).
[31] T. Kuschel, T. Becker, D. Bruns, M. Suendorf, F. Bertram, P. Fumagalli, and J. Wollschläger, J. Appl. Phys. **109**, 093907 (2011).
[32] P. F. Carcia, A. D. Meinhaldt, and A. Suna, Appl. Phys. Lett. **47**, 178 (1985).
[33] C. Kittel, Phys. Rev. **70**, 965 (1946).